THE TIMING OF PHAGE DNA REPLICATION INFLUENCES CELLULAR DECISION-MAKING

An Undergraduate Research Scholars Thesis

by

JAMES ETHAN CORBAN

Submitted to the Undergraduate Research Scholars program at
Texas A&M University
in partial fulfillment of the requirements for the designation as an

UNDERGRADUATE RESEARCH SCHOLAR

Approved by Research Advisor: Dr. Lanying Zeng

May 2020

Major: Biochemistry
Genetics

TABLE OF CONTENTS

ABSTRACT

The Timing of Phage DNA Replication Influences Cellular Decision-making

James Corban
Department of Biochemistry and Biophysics
Texas A&M University

Research Advisor: Dr. Lanying Zeng
Department of Biochemistry and Biophysics
Texas A&M University

In this study, we use the bacteriophage lambda and *E. coli* model system to examine the effects of lambda DNA replication on the lysis-lysogeny decision. In the lytic pathway, lambda's structural and lysis genes are rapidly transcribed and translated, culminating with the burst of the host cell and release of ~one hundred progeny virions which conduct further infection cycles. The temperate lysogenic pathway consists of the integration of the lambda genome into the host chromosome and the maintenance of stable, replicating lysogenic cells via the repression of lambda lysis and replication genes. We employ nalidixic acid (NA), a quinolone antibiotic, as an inhibitory agent to lambda DNA replication. NA inhibits DNA gyrase, leading to the buildup of positive supercoiling stress ahead of replication forks and a stall in DNA replication. Both *E. coli* and phage lambda rely on DNA gyrase for maintaining their respective DNA molecules in proper supercoiled states to facilitate DNA replication. In this work, we determine that a delay to the start of lambda DNA replication significantly affects decision-making in the lysis-lysogeny system and we discuss the mechanisms which could lead to the altered outcomes. We also examine an alternate method of altering lambda DNA replication by controlling the production of lambda-specific DNA replication proteins, a protein critical specifically for initiating the

replication of lambda DNA molecules. By infecting cells which may be induced to express O or P with lambda mutants which are deficient for that protein, we could potentially observe variances in the lysis-lysogeny decision at distinct DNA replication rates.

ACKNOWLEDGMENTS

The work in this study was performed with the much appreciated support and guidance of Dr. Lanying Zeng as well as graduate students in the Zeng lab.

CHAPTER I

INTRODUCTION

Ubiquitous in biological systems, cellular decision-making describes the process by which distinct phenotypic outcomes result from the varied expression of genes along regulatory cascades (1). Decision-making at the single-cell level can be magnified within cellular populations, which in many cases (such as sporulation, apoptosis, or tumorigenesis) translate to significant impacts on the health and behavior of multicellular organisms (2, 3). Numerous intra- and extracellular factors can contribute to gene expression involved in cellular decision-making, including environmental conditions (temperature, pressure, etc.), nutrient availability, population density, or the abundance of transcriptional or translational regulators (1, 4). DNA copy number fluctuation via DNA replication is a factor in gene expression experienced to varying degrees by nearly every biological system (1). Increased gene dosage could amplify the expression of a given gene while decreased gene dosage could dampen expression, with either eventuality subjecting organisms to altered phenotypes (1, 5). Diverse regulatory responses can tune the sensitivity or robustness of gene networks to DNA copy number changes to achieve the optimal phenotypic outcome for the organism (or its population) (6). Investigating the effects of altered DNA replication patterns (and the resultant DNA copy number fluctuation) on cellular decision-making outcomes may provide valuable insight into the role of gene dosage on regulatory network expression.

In this work, we study the bacteriophage lambda and *E. coli* infection cycle to examine the effects of altered lambda DNA replication on the lysis-lysogeny decision. The lambda lysis-lysogeny decision, often referred to as the “genetic switch”, stands as one of the most well-

defined models of cellular decision-making (7). In the lytic pathway, lambda's structural and lysis genes are rapidly transcribed and translated, culminating with the burst of the host cell and release of several hundred progeny virions which conduct further infection cycles (7). The comparatively temperate lysogenic pathway consists of the integration of the lambda genome into the host chromosome and the maintenance of stable, replicating lysogenic cells via the repression of lambda lysis and replication genes (7). Past studies have demonstrated that phage lambda DNA replication is integral to the lysis-lysogeny decision (1, 8).

We employed two separate strategies to alter lambda DNA replication patterns during the infection process. Nalidixic acid (NA), a quinolone antibiotic, was used as an inhibitory agent to lambda DNA replication (9). NA targets DNA gyrase and inhibits the enzyme's nicking-closing activity, leading to the buildup of positive supercoiling stress ahead of replication forks and a stall in DNA replication (9). Both *E. coli* and phage lambda rely on DNA gyrase for maintaining their respective DNA molecules in proper supercoiled states to facilitate DNA replication. We applied concentrations of NA with negligible effects on *E. coli* viability to examine the impact of NA treatment on lambda DNA replication and the lysis-lysogeny decision. The second strategy used to alter lambda DNA replication centered on controlling the production of lambda replication proteins, O and P. The lambda O protein functions similarly to DnaA in *E. coli*: a sufficient accumulation of O triggers the opening of lambda's replication fork and allows for replication to begin (10). P interacts with host DnaB and shuttles the protein to the lambda replication fork to facilitate opening of the double-stranded lambda genome (11). Cells containing plasmids inducible for P or O expression were infected with P or O (respectively) deficient lambda mutants.

Our study indicates that a delay to the start of lambda DNA replication significantly affects decision-making in the lysis-lysogeny system and we discuss the mechanisms which could lead to the altered phenotypic outcomes. Future studies will provide a greater level of clarity on the impact of controlled P or O expression on lambda decision-making.

CHAPTER II

METHODS

Strains, Plasmids, and Phages

The host *E. coli* strain for the normal single-cell infection assays and qPCR analysis was MG1655. The host used for single-cell phage DNA copy number tracking assays was MG1655 *pACYC177-PFtsKi-tetR-mNeonGreen*.

The plasmids *pBAD33* (12) and *pZS*24* (13) each expressing P were transformed into a MG1655 *lacY*-*lacIQ* strain (MG1655 *lacY*-*lacIQ-pBAD33-P* and MG1655 *lacY*-*lacIQ-pZS*24-P*). Similarly, *pBAD33* and *pZS*24* each expressing O were transformed into MG1655 *lacY*-*lacIQ* (MG1655 *lacY*-*lacIQ-pBAD33-O* and MG1655 *lacY*-*lacIQ-pZS*24-O*).

The reporter phage for normal single-cell infection assays was *λD-mTurquoise2 cI857-mKO2 bor::Cm*^{R} (8) (Fig. 1). Phage *λD-mTurquoise2 cI857-mKO2 bor::48xtetO Cm*^{R} was used for single-cell DNA copy number tracking movies. The phage used in qPCR analysis was *λcI857 bor::Kan*^{R}. λP- phage (*λcI857 Pam80 bor::Kan*^{R}) was used for infections of MG1655 *lacY*-*lacIQ-pBAD33-P* and MG1655 *lacY*-*lacIQ-pZS*24-P* strains. All phages were purified as previously described (8).

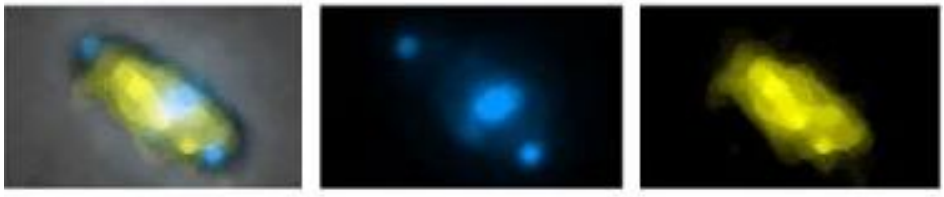

Figure 1: A cell infected with *λD-mTurquoise2 cI857-mKO2 bor::Cm*^{R} expressing both lytic and lysogenic activity (referred to in this study as "mixed-fate" cells) (8). Lytic expression: gpD-mTurq2 (blue). Lysogenic expression: *cI*-mKO2 (yellow).

DNA Quantification at Bulk-Level via qPCR

One mL overnight culture of *E. coli* MG1655, grown at 37°C in M9MM (M9 minimal media + 0.4% maltose + 10 mM $MgSO_4$) with 265 rpm shaking, was diluted 1:100 into 20 mL M9MM. The culture was grown at 37°C with 265 rpm shaking to OD_{600} ~0.4. The cells were collected by centrifugation (2000*g*, 4°C, 15 min), the supernatant was discarded, and the pellet was resuspended with 1:10 volume of fresh ice-cold M9MM. An appropriate amount of *λ*LZ613 was added to the sample to reach a target API of 2 (average phage infection, e.g. the average infected cell is infected by two phages), with pipetting to mix. The cell+phage mixture was incubated on ice for 30 minutes to allow for phage adsorption. While the sample was on ice, 1.8 mL of M9GM (M9 + 0.2% glucose + 10 mM $MgSO_4$) was added to six new falcon tubes (for 20, 40, 60, 80, 100, and 120-minute samples). The six M9GM tubes were pre-warmed in a 30°C water bath. Seven 15 mL centrifuge tubes were filled with two mL of methanol and stored at -20°C. An ethanol-dry ice slurry was prepared with sufficient depth to submerge a 15 mL centrifuge tube to the four mL mark. The cell+phage mixture was transferred to a 35°C water bath and incubated for five minutes. The sample was immediately diluted by adding 200 µL to each of the six M9GM tubes prewarmed at 30°C. For the 0-minute sample, 200 µL was added directly to two mL chilled methanol and immediately placed in the ethanol-dry ice slurry to freeze. The six M9GM sample tubes were incubated at 30°C with 225 rpm shaking, with one sample being transferred to the ethanol-dry ice slurry every 20 minutes up to a final time point of 120 minutes. After being left in the ethanol-dry ice slurry for two minutes, each sample was centrifuged (4000*g*, 4°C, 10 min) and the methanol was discarded. The remaining pellet for each sample was stored at -20°C.

DNA extraction for each sample was performed with the UltraClean Microbial DNA Isolation Kit (MO BIO Laboratories, #12224-50) following standard protocols. SYBR Green PCR master mix was used for DNA detection. For each sample, primers targeting the phage genome were used to quantify phage DNA, while *E. coli* DNA was quantified using primers which targeted the *dxs* gene (Table 1) (1).

Table 1. Primers used for qPCR experiments which target *E. coli* or phage lambda DNA.

E. coli dxs forward primer	*E. coli dxs* reverse primer	Lambda *E* forward primer	Lambda *E* reverse primer
5'-CGAGAAACTGGCGATCCTTA	5'- CTTCATCAAGCGGTTTCACA	5'- CTGGGTGAACAACTGAACCG	5'- ATCCGTGTCATCAAGCTCCT

Single-cell Infection Assay

One mL of overnight culture of MG1655 (grown in M9M at 37°C with 265 rpm shaking) was diluted 1:100 into M9M. The culture was grown at 37°C with 265 rpm to OD_{600} ~0.4. 1 mL of the grown culture was collected in a microcentrifuge tube and centrifuged (4000*g*, 4 min), the supernatant was discarded, and the pellet was resuspended in 1:10 volume of fresh ice-cold M9M (for experiments with NA, the pellet was resuspended in 1:10 volume of ice-cold M9M with 2x final NA concentration). 20 μL of the cells was transferred to a separate microcentrifuge tube and mixed (by gentle pipetting) with 20 μL of phage at an appropriate titer. The cell+phage mixture was incubated on ice for 30 minutes. A separate tube was prepared with 40 μL M9M (for experiments with NA, used 40 μL M9M with 1x final NA concentration) and left at room temperature. The cell+phage mixture was incubated in a 35°C water bath for five minutes. While waiting, a small 1.5% agarose M9M pad was placed onto an 18x18mm Fisher Scientific coverslip. 10 μL of the cell+phage mixture was transferred (with a pipette tip cut to provide a larger opening) to the tube containing 40 μL M9M and lightly tapped to mix. Next, 1 μL of the

sample was pipetted (with a cut pipette tip) onto the M9M pad. After the sample was dried (~one minute), a 24x50mm Fisher Scientific coverslip was placed onto the M9M pad, and the sample was imaged by microscope following previously established protocols (8).

CHAPTER III

RESULTS

Effects of Nalidixic Acid Treatment on *E. coli* MG1655 Viability

Preliminary experiments were performed to determine working NA concentrations at which delayed lambda DNA replication was observed with negligible impacts on *E. coli* MG1655 viability. Single-cell analysis of infected cells (from fluorescence microscopy imaging) grown in the presence of 10 μg/mL NA demonstrated no apparent increase in death rates (excluding deaths due to lytic events). Cells treated with 20 μg/mL NA demonstrated only mildly increased death rates (~5-10% higher) at MOI 0-2. To verify that NA treatment at 10 and 20 μg/mL did not interfere with ejection of phage DNA into the cell or block lambda lysis-lysogeny gene expression, the failed infection rates (cells with visibly adsorbed phages exhibiting no lytic-lysogenic activity) of NA treatment groups were measured. No significant variations in failed infection rates were detected at any MOI for the NA treatment groups as compared to infected cells grown in the absence of NA.

Nalidixic Acid Treatment Corresponds with Delayed Lambda DNA Replication

We quantified phage DNA levels in populations of infected cells with and without NA treatment over time (Fig.2). A distinct delay in phage DNA replication was observed, distinguishable at the 20-minute time point in Fig.2a. This delay appeared complete: no increase in phage DNA fold change was detected. By taking the log of the fold change values (excluding the 0-minute point for the NA treatment groups) and comparing the slope values for each dataset, the rate of phage DNA replication in the NA treatment groups following the delay was found to be essentially unchanged as compared to the control group.

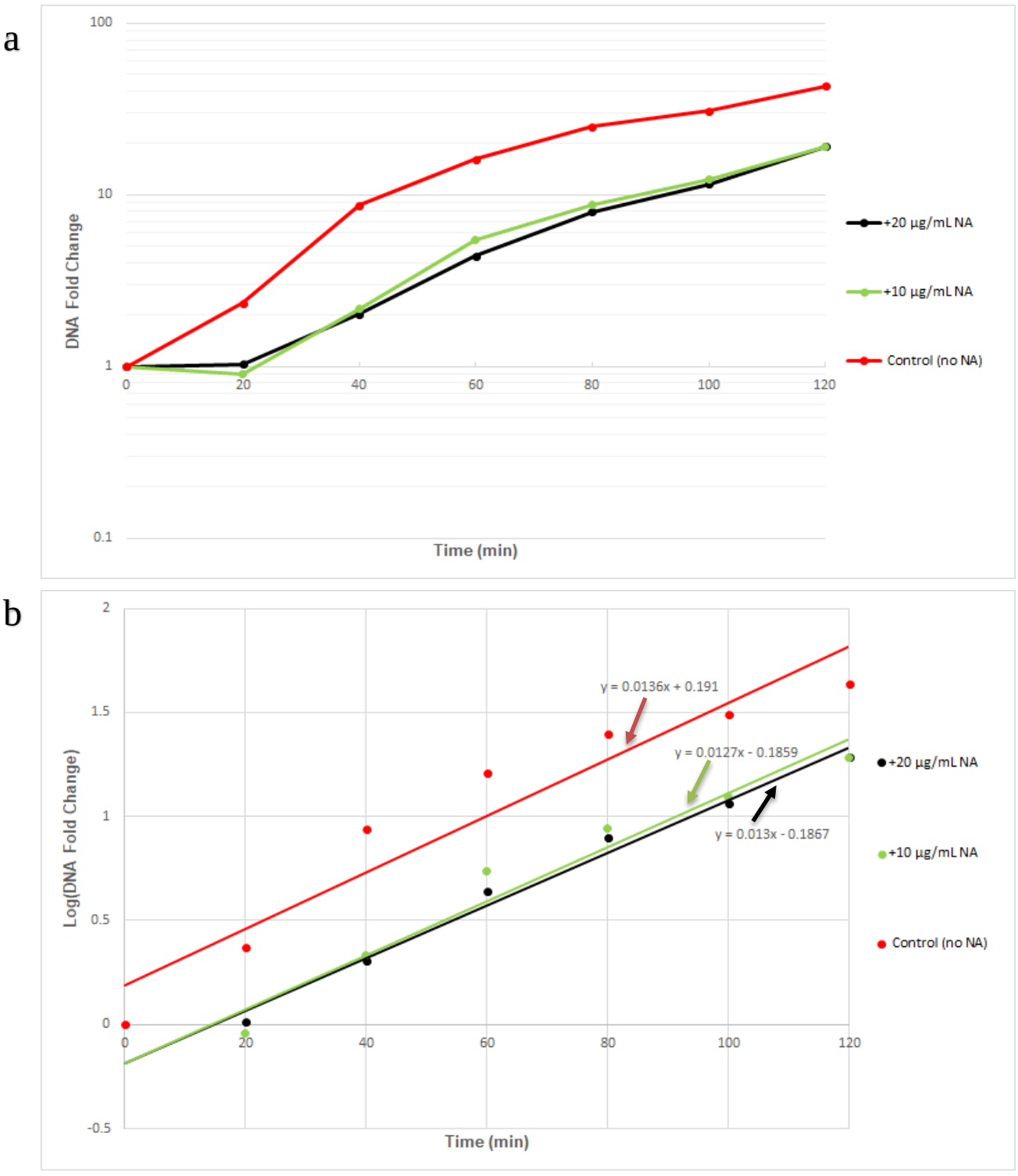

Figure 2: Data for each treatment group represents average of three separate qPCR trials. **(a)** Phage lambda DNA levels in infected *E. coli* cells over time as detected via qPCR. Fold change calculated as ratio of phage DNA over *E. coli* DNA in each treatment group and normalized to the ratio measured at 0 min. **(b)** Log of DNA levels given in Fig. 2a. Rates of phage DNA replication for each treatment group represented by values of linear trendline slopes (indicated by arrows).

Next, we sought to visualize the observed delay in phage DNA replication at the single-cell level via the application of a tetracycline expression system (10). An MG1655 strain was transformed with a multi-copy number plasmid constitutively expressing TetR protein fused with the fluorescent protein mNeongreen. A phage was constructed with 48 *tetO* regions which are selectively recognized by TetR. Upon injection of phage DNA into the host cell, TetR-mNeongreen binds to the *tetO* regions. By visualizing the mNeongreen fluorescence signal, clusters of phage DNA can be tracked via time-lapse microscope imaging. Once background mNeongreen fluorescence intensity is subtracted, the fluorescence intensity produced by a single phage DNA molecule can be used as a baseline by which to quantify phage DNA copy number over time in infected cells (e.g. 20x the signal associated with a single phage DNA molecule would represent 20 phage DNA molecules). Representative time-lapse images of a *tetO*-TetR infection are shown in Fig.3. The MATLAB script with which we are analyzing *teto*-TetR-mNeongreen image data remains under development, although preliminary results appear to corroborate the delayed start to phage DNA replication observed via bulk-level DNA quantification.

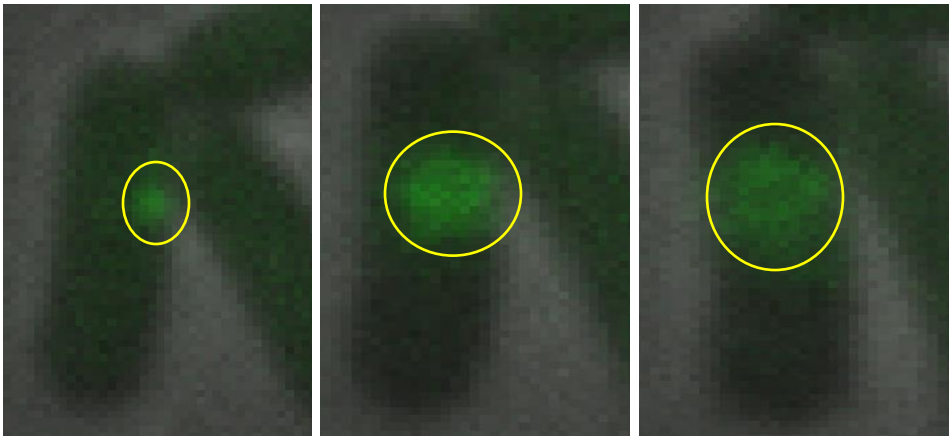

Figure 3: Images taken from a time-lapse infection movie using the *tetO*-TetR-mNeongreen system (0 minute image is taken approximately 15 minutes post phage injection into cell). The green fluorescence bordered by yellow indicates phage DNA labeled with TetR-mNeongreen.

Delayed Lambda DNA Replication Impacts Lysis-Lysogeny Decision

Phage lambda decision-making was assayed at the single-cell level via fluorescence imaging with two fluorescent proteins used as our reporters: mTurquoise2 and mKO2 (Fig.5) (8). The *mTurquoise2* gene was translationally fused to the *λD* gene, which encodes the capsid decoration protein gpD (present in several hundred copies on each capsid) (8). Therefore, mTurquoise2 signal allowed for the detection of lytic activity (via the labeling of assembling phages in lytic cells) and the quantification of infecting phages for each cell (8). The *mKO2* gene was transcriptionally fused downstream of *cI* to function as a lysogeny reporter, with mKO2 expressed as a separate protein so as to avoid interfering with CI activity (8). The *cI* operon is expressed during the establishment and maintenance of lysogeny (7). All infections for microscopy imaging were performed in M9M (M9 minimal media + 0.4% maltose) media to optimize the measurement of fluorescent signals.

The percentage of infected cells expressing pure lytic activity (i.e. no lysogenic signal) was significantly reduced in the NA treatment groups, especially at low MOI (Fig.4a). At MOIs of 1 and 2, pure lysis percentage was reduced by 30-50% with NA treatment. As expected, lysogeny rates increased with MOI for infected cells grown with and without NA (Fig.4b) (8). Relative to the control, a higher percentage of lysogeny was observed for NA at low MOI (1-2) and a lower percentage was observed at high MOI (3-4). Most notably, a sharp increase in the percentage of mixed fate cells (expressing both lytic and lysogenic activity) was observed with NA treatment (Fig.4c). Between 35-50% of infected cells in the NA treatment groups were mixed at MOI 1-4, as compared to ≤10% at MOI 1-4 in the control. NA treatment also corresponded with significantly delayed lysis times. As compared to the control cells, the

average lysis time was delayed by 85 minutes with 10 µg/mL NA and 110 minutes with 20 µg/mL NA (Fig.4d).

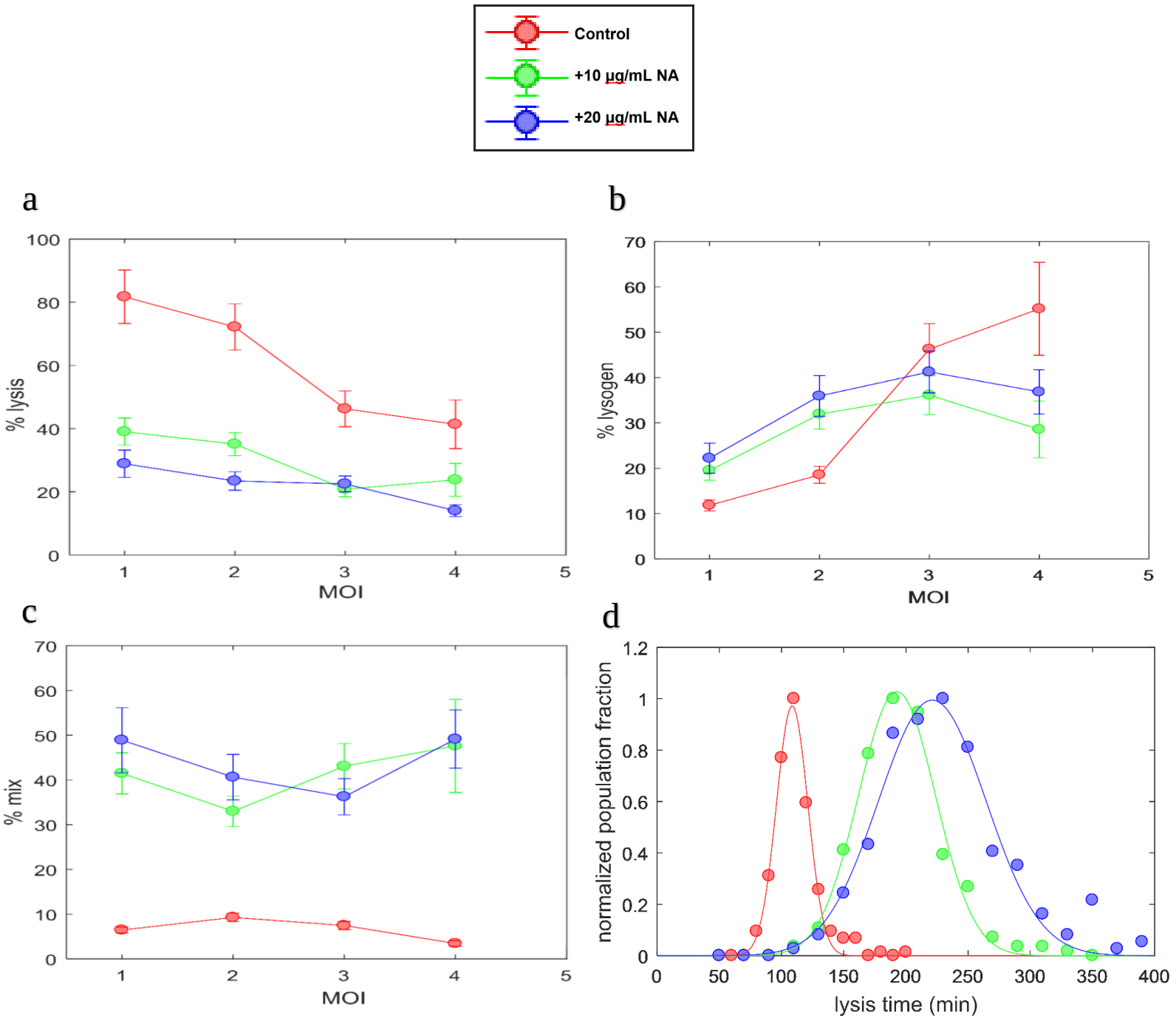

Figure 4: Single-cell infection data from fluorescence microscopy imaging. **(a)** Percentage of infected cells expressing pure lysogenic activity. **(b)** Percentage of infected cells expressing pure lytic activity. **(c)** Percentage of infected cells expressing both lytic and lysogenic activity ("mixed" fate cells). **(d)** Fraction of total lytic cells (pure lytic + mixed) which lysed at given time points.

Impact of Controlled P and O Protein Expression on Lambda Lysis-Lysogeny Decision

E. coli strains were transformed with plasmids which inducibly express O or P. These strains will be infected by lambda phages deficient for O or P expression. The bulk-level DNA quantification of these infected cells will be quantified via qPCR (with results depicted in the same format as displayed in Fig.2). These results will determine if: (a) the rate of lambda DNA replication is lowered in infections with O/P deficient phages; (b) O/P deficient lambda DNA replication can be fully recovered with sufficient O/P expression from their host strains; (c) if overexpression of O/P can increase lambda DNA replication relative to that of wild type infections. If the bulk-level DNA quantification results indicate that the lambda DNA replication rate was lowered relative to the control group (cells infected with wild-type lambda), then single-cell fluorescence infection assays will be performed (as previously described) to quantify phage DNA at the single cell level over time (via the *tetO*-TetR-mNeongreen method, Fig.5) and to determine whether the altered DNA replication rates impact the frequencies of lysis-lysogeny decision outcomes. Due to the events surrounding the COVID-19 virus in the spring of 2020, these experiments and their corresponding results were unavailable at the time of publication for this URS thesis.

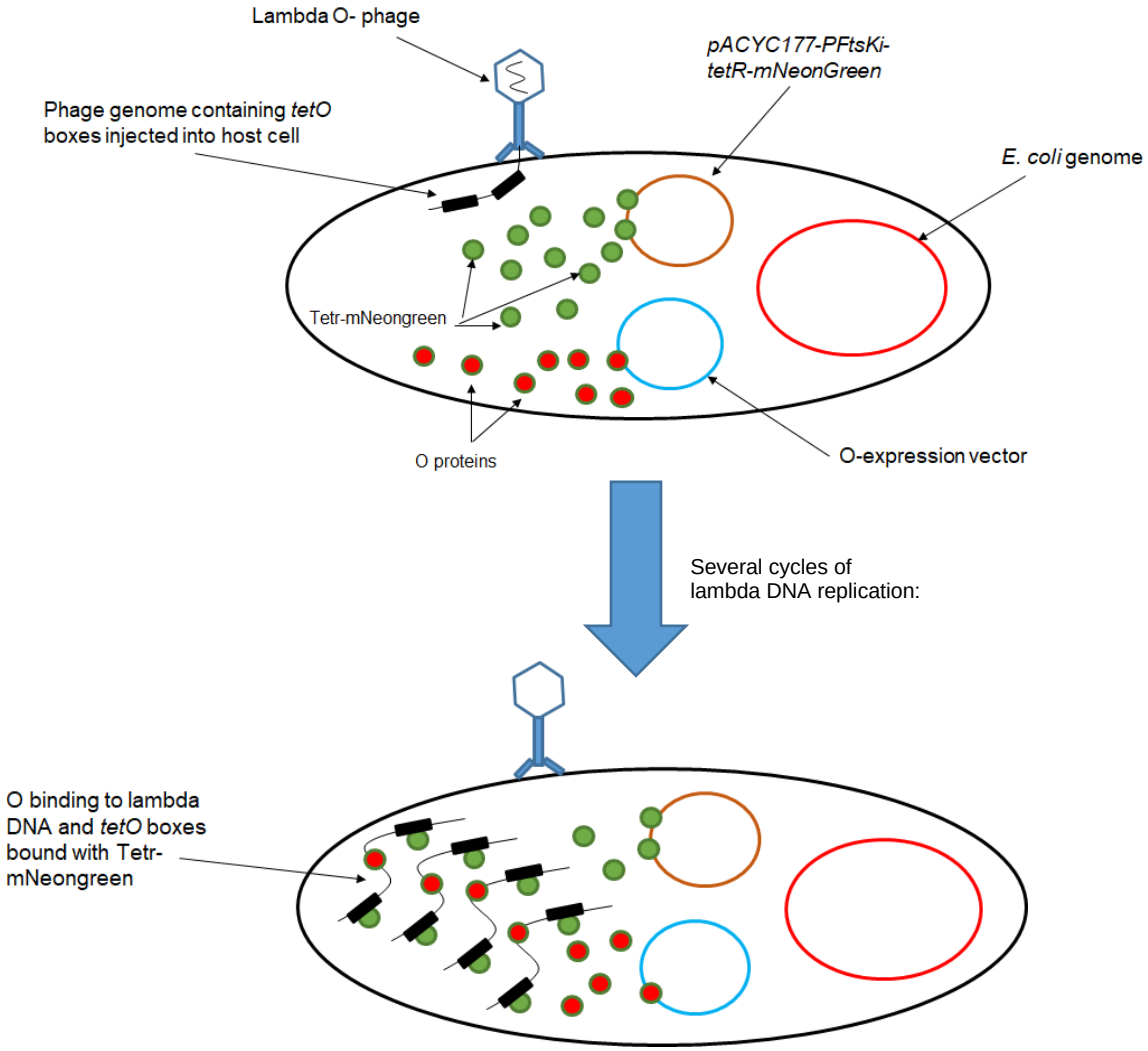

Figure 5: Graphic representation of *tetO*-Tetr-mNeongreen array which will be used to quantify phage DNA levels over time at the single-cell level in cells expressing O infected with O-deficient phages. The increase in phage DNA can be measured in relation to elevations in fluorescence intensity over time. Infection of cells inducibly expressing O (a lambda specific DNA replication protein) with lambda O- phages will allow for controlled rates of replication. An identical approach to this figure will be used for the inducible expression of P.

CHAPTER IV

CONCLUSION

Insights gained from the study of cellular decision-making mechanisms within model biological systems such as phage lambda are necessary for understanding critical processes including organismal development and disease progression (1). In this work, nalidixic acid was identified as a lambda DNA replication delay agent and the corresponding effects of this delay on the lysis-lysogeny decision were examined.

Following the observed delay to the start of phage DNA replication, the rate of phage DNA replication in the NA treatment groups closely reflected that of the control group. While the precise explanation behind this outcome has not yet been determined, certain factors have been hypothesized to be involved. Upon injection into the host cell, lambda DNA first undergoes several cycles of theta replication. The theta mode of replication consists of bidirectional replication initiated from the *oriλ* site and produces daughter circles of the phage genome (14). Late-stage DNA replication (~15 minutes post-infection in ideal lysis conditions) involves the switch from theta to sigma, or rolling-circle, replication (14). The sigma mode consists of unidirectional replication and the creation of long, linear dsDNA concatemers of the phage genome (14). The precise mechanism of the replication mode switch remains unconfirmed. Previous studies have demonstrated that continued transcription at *oriλ* corresponds with bidirectional replication, while stalls in transcription lead to a subsequent switch to unidirectional sigma replication (14, 15). We hypothesize that the observed delay in phage DNA replication may be associated with the theta/sigma replication switch. As stated previously, NA inhibits DNA replication by creating a buildup of positive supercoiling stress ahead of replication forks. The stress buildup may inhibit transcription at *oriλ*, leading to a switch to sigma replication. The

inhibitory effect of the increased positive supercoiling stress on the rate of phage DNA replication may be lessened when the DNA is being replicated unidirectionally in a linear dsDNA format (sigma), as opposed to bidirectionally in a circular dsDNA format (theta). Therefore, a delay in replication would be observed during early replication (while in theta mode) while replication may return to a normal rate in late replication (sigma mode).

The most dramatic difference observed in the lysis-lysogeny decision due to a delay in phage DNA replication was a substantial increase in mixed fate cells. This outcome could be due to a buildup of the lambda transcriptional repressors Cro and CI (or specifically, an accumulation of CII which transcriptionally activates *cI*) during delayed replication (7). Cro binding is associated with lytic activity, while CI binding is associated with lysogenic activity. These two proteins compete with each other for the same binding sites, and whichever protein "wins" the contest switches the lysis-lysogeny circuit to commit to the victor's pathway while repressing the activity of the loser (e.g., if Cro "wins", lysis and replication genes are rapidly transcribed while genes associated with lysogeny are repressed) (15). With delayed replication, CI and Cro would continue to accumulate while the number of phage genomes remained the same. Upon the switch to increased phage DNA replication, a surge in lambda DNA could generate a rapid binding competition between latent pools of Cro and CI. This could confuse the normal lysis-lysogeny decision and contribute to the observed increase in combined lytic and lysogenic activity in infected cells. A prominent factor in the delayed lysis times observed for the NA treatment groups was most likely the greatly increased proportion of mixed cells in those groups. As demonstrated in previous studies, cells expressing both lytic and lysogenic activity experience "confusion" and result in delayed lysis times (8).

In future studies, we intend to refine the *tetO*-TetR-mNeongreen method used for the tracking and quantification of phage DNA copy number within infected cells. A significant problem we encountered while quantifying phage DNA copy number via time-lapse microscopy was that the actual mNeongreen signal may be partially obscured or difficult to visualize depending on the 3-D organization of the DNA molecules at any given time point. As a result, measured fluorescence signals could be higher or lower than their true value. To remedy this, additional time-lapse movies were performed with five z-stack (+/- 0.6 μm with spacing of 0.3 μm) images at each stage. The MATLAB script we will use to analyze data from these z-stack movies is currently being optimized. Ideally, analysis of the *tetO*-tetR-mNeongreen movies will both verify our observed delay in phage DNA replication and allow us to visualize any resultant alteration to phage DNA localization within the cell. Additionally, bulk-level and single-cell level DNA quantification will be performed on O/P expressing *E. coli* strains infected with O/P deficient lambda phages to verify whether controlled O/P expression can lower or (with sufficient expression) raise the rate of lambda DNA replication. Single-cell fluorescence infection assays with O/P deficient phages will be performed to demonstrate the impact of altered DNA replication on lysis-lysogeny decision outcomes.

REFERENCES

1. Shao Q, Cortes MG, Trinh JT, Guan J, Balazsi G, Zeng L. 2018. Coupling of DNA Replication and Negative Feedback Controls Gene Expression for Cell-Fate Decisions. iScience 6:1-12.

2. Balazsi G, van Oudenaarden A, Collins JJ. 2011. Cellular decision making and biological noise: from microbes to mammals. Cell 144:910-25.

3. Zhou JX, Brusch L, Huang S. 2011. Predicting pancreas cell fate decisions and reprogramming with a hierarchical multi-attractor model. PLoS One 6:e14752.

4. Gonzalez C, Ray JC, Manhart M, Adams RM, Nevozhay D, Morozov AV, Balazsi G. 2015. Stress-response balance drives the evolution of a network module and its host genome. Mol Syst Biol 11:827.

5. Mileyko Y, Joh RI, Weitz JS. 2008. Small-scale copy number variation and largescale changes in gene expression. Proc Natl Acad Sci USA 105:16659-64.

6. M.W. K. 2010. A general lack of compensation for gene dosage in yeast. Mol Syst Biol 6.

7. Ptashne M. 2004. A Genetic Switch: Phage Lambda Revisited Cold Spring Harbor Press.

8. Trinh JT, Székely T, Shao Q, Balázsi G, Zeng L. 2017. Cell fate decisions emerge as phages cooperate or compete inside their host. Nature Communications 8:14341.

9. Pommier Y, Leo E, Zhang H, Marchand C. 2010. DNA topoisomerases and their poisoning by anticancer and antibacterial drugs. Chem Biol 17:421-33.

10. Rajagopala SV, Casjens S, Uetz P. 2011. The protein interaction map of bacteriophage lambda. BMC Microbiol. 11:213-213.

11. Hayes S, et al. 2013. Phage Lambda P Protein: Trans-Activation, Inhibition Phenotypes and Their Suppression. Viruses, MDPI.

12. Guzman LM, Belin D, Carson MJ, Beckwith J. 1995. Tight regulation, modulation, and high-level expression by vectors containing the arabinose PBAD promoter. J Bacteriol. 177(14):4121-30.

13. Nistala JG, Wu K, Rao VC, Bhalerao DK. 2010. A modular positive feedback-based gene amplifier. J Biol Eng. 4: 4.

14. Narajczyk M, Baranska S, Wegrzyn A, Wegrzyn G. 2007. Switch from theta to sigma replication of bacteriophage lambda DNA: factors involved in the process and a model for its regulation. Mol Genet Genomics 278:65-74.

15. Baranska S, Gabig M, Wegrzyn A, Konopa G, Herman-Antosiewicz A, Hernandez P, Schvartzman JB, Helinski DR, Wegrzyn G. 2001. Regulation of the switch from early to late bacteriophage lambda DNA replication. Microbiology 147:535-47.